doi:10.1093/brain/awab148 BRAIN 2021: 144; 2696–2708 | 2696

BRAIN
ORIGINAL ARTICLE

COVID-19 neuropathology at Columbia University Irving Medical Center/New York Presbyterian Hospital

Kiran T. Thakur,[1,†] Emily Happy Miller,[2,†] Michael D. Glendinning,[1] Osama Al-Dalahmah,[3] Matei A. Banu,[4] Amelia K. Boehme,[1] Alexandra L. Boubour,[1] Samuel S. Bruce,[1] Alexander M. Chong,[2] Jan Claassen,[1] Phyllis L. Faust,[3] Gunnar Hargus,[3] Richard A. Hickman,[3] Sachin Jambawalikar,[5] Alexander G. Khandji,[5] Carla Y. Kim,[1] Robyn S. Klein,[6] Angela Lignelli-Dipple,[5] Chun-Chieh Lin,[7] Yang Liu,[3] Michael L. Miller,[3] Gul Moonis,[5] Anna S. Nordvig,[1] Jonathan B. Overdevest,[8] Morgan L. Prust,[1] Serge Przedborski,[1,3,9] William H. Roth,[1] Allison Soung,[6] Kurenai Tanji,[3] Andrew F. Teich,[3] Dritan Agalliu,[1,3,‡] Anne-Catrin Uhlemann,[2,‡] James E. Goldman[3,‡] and Peter Canoll[3,‡]

[†,‡]These authors contributed equally to this work.

Many patients with SARS-CoV-2 infection develop neurological signs and symptoms; although, to date, little evidence exists that primary infection of the brain is a significant contributing factor. We present the clinical, neuropathological and molecular findings of 41 consecutive patients with SARS-CoV-2 infections who died and underwent autopsy in our medical centre. The mean age was 74 years (38–97 years), 27 patients (66%) were male and 34 (83%) were of Hispanic/Latinx ethnicity.

Twenty-four patients (59%) were admitted to the intensive care unit. Hospital-associated complications were common, including eight patients (20%) with deep vein thrombosis/pulmonary embolism, seven (17%) with acute kidney injury requiring dialysis and 10 (24%) with positive blood cultures during admission. Eight (20%) patients died within 24 h of hospital admission, while 11 (27%) died more than 4 weeks after hospital admission. Neuropathological examination of 20–30 areas from each brain revealed hypoxic/ischaemic changes in all brains, both global and focal; large and small infarcts, many of which appeared haemorrhagic; and microglial activation with microglial nodules accompanied by neuronophagia, most prominently in the brainstem.

We observed sparse T lymphocyte accumulation in either perivascular regions or in the brain parenchyma. Many brains contained atherosclerosis of large arteries and arteriolosclerosis, although none showed evidence of vasculitis. Eighteen patients (44%) exhibited pathologies of neurodegenerative diseases, which was not unexpected given the age range of our patients. We examined multiple fresh frozen and fixed tissues from 28 brains for the presence of viral RNA and protein, using quantitative reverse-transcriptase PCR, RNAscope® and immunocytochemistry with primers, probes and antibodies directed against the spike and nucleocapsid regions.

The PCR analysis revealed low to very low, but detectable, viral RNA levels in the majority of brains, although they were far lower than those in the nasal epithelia. RNAscope® and immunocytochemistry failed to detect viral RNA or protein in brains. Our findings indicate that the levels of detectable virus in coronavirus disease 2019 brains are very low and do not correlate with the histopathological alterations. These findings suggest that microglial activation,

Received December 05, 2020. Revised March 17, 2021. Accepted March 20, 2021. Advance access publication April 15, 2021

microglial nodules and neuronophagia, observed in the majority of brains, do not result from direct viral infection of brain parenchyma, but more likely from systemic inflammation, perhaps with synergistic contribution from hypoxia/ischaemia. Further studies are needed to define whether these pathologies, if present in patients who survive coronavirus disease 2019, might contribute to chronic neurological problems.

1 Department of Neurology, Vagelos College of Physicians and Surgeons, Columbia University Irving Medical Center, and the New York Presbyterian Hospital, New York, NY 10032, USA
2 Department of Medicine, Division of Infectious Diseases, Vagelos College of Physicians and Surgeons, Columbia University Irving Medical Center, and the NewYork Presbyterian Hospital, New York, NY 10032, USA
3 Department of Pathology and Cell Biology, Division of Neuropathology, Vagelos College of Physicians and Surgeons, Columbia University Irving Medical Center, and the New York Presbyterian Hospital, New York, NY 10032, USA
4 Department of Neurological Surgery, Vagelos College of Physicians and Surgeons, Columbia University Irving Medical Center, and the New York Presbyterian Hospital, New York, NY 10032, USA
5 Department of Radiology, Vagelos College of Physicians and Surgeons, Columbia University Irving Medical Center, and the New York Presbyterian Hospital, New York, NY 10032, USA
6 Departments of Medicine, Pathology and Immunology, Neurosciences, Washington University School of Medicine, St. Louis, MO 63110, USA
7 Department of Pathology and Laboratory Medicine, Dartmouth-Hitchcock Medical Center, Lebanon, NH 03756, USA
8 Department of Otolaryngology, Vagelos College of Physicians and Surgeons, Columbia University Irving Medical Center, The New York Presbyterian Hospital, New York, NY 10032, USA
9 Department of Neuroscience, Vagelos College of Physicians and Surgeons, Columbia University Irving Medical Center, and the New York Presbyterian Hospital, New York, NY 10032, USA

Correspondence to: Peter Canoll, MD, PhD
Department of Pathology and Cell Biology, Division of Neuropathology
Vagelos College of Physicians and Surgeons
Columbia University Irving Medical Center and the New York Presbyterian Hospital
630 W. 168th Street New York, NY, 10032, USA
E-mail: pc561@cumc.columbia.edu

Keywords: COVID-19; SARS-CoV-2; neuropathology; microglia activation; microglial nodules

Abbreviations: COVID-19 = coronavirus disease 2019; HSV-1 = herpes simplex virus type 1; N = nucleocapsid; SARS-CoV-2 = severe acute respiratory syndrome coronavirus 2

Introduction

Neurological manifestations of severe acute respiratory syndrome coronavirus 2 (SARS-CoV-2) infection are increasingly recognized[1] and include seizures,[2,3] cerebrovascular accidents,[4–8] encephalopathy,[7] isolated cases of acute necrotizing haemorrhagic encephalopathy[9] and Guillain-Barré syndrome.[10] Many of the neurological conditions seen in the context of SARS-CoV-2 infection are associated with systemic effects, including multiorgan damage, hypercoagulability and a proinflammatory state.[11–14] Whether SARS-CoV-2 directly infects the brain remains controversial. Related β-coronaviruses such as severe acute respiratory syndrome (SARS) and Middle East respiratory syndrome (MERS) show neuro-invasive potential,[1,15–17] and clinicians have reported cases of meningoencephalitis in coronavirus disease 2019 (COVID-19) patients, without neuropathological confirmation.[3,16,18–23] Further characterization of the neuropathological and molecular findings in COVID-19 brains is needed to understand the pathophysiological mechanisms underlying the neurological conditions seen in the context of COVID-19.

A few autopsy studies have reported the neuropathological findings of patients with SARS-CoV-2 infections (Supplementary Table 1), including hypoxic changes, vascular lesions, demyelinating pathology resembling acute disseminated encephalomyelitis,[24] reactive astrocytosis and microgliosis[25] and cerebral haemorrhage or haemorrhagic suffusion.[26] Viral RNA has been detected at low levels by quantitative reverse transcriptase-PCR (qRT-PCR) in some cases,[27–29] but evidence directly linking virus to the COVID-associated neuropathology is controversial. We present the neuropathological findings of 41 consecutive patients with histories of confirmed SARS-CoV-2 infection, investigating the clinical and pathological characteristics.

Materials and methods

This study was approved by the Columbia University Irving Medical Center (CUIMC) Institutional Review Board and is in line with the Declaration of Helsinki. The requirement for written informed consent for chart review was waived as the study design was deemed to cause no more than minimal risk. The Institutional Review Board approved this study (AAAS9987) on 4 May 2020.

Consent for autopsy was obtained from patient surrogates through standardized consenting procedures via telephone, given that no visitors were allowed in hospital during the study time. We included all consecutive autopsies with brain removal starting during the fourth week of March 2020 and ending in the third week of June 2020. All cases met the Centre for Disease Control and Prevention case definition for definitive COVID-19 infection (https://ndc.services.cdc.gov/). Clinical data including demographics, clinical, laboratory, radiographic and treatment data were obtained retrospectively through an electronic medical record review. All laboratory tests, neuroradiology assessments and interventions were performed at the discretion of the treating physicians.

Autopsy procedures

All autopsies were conducted in a negative pressure room. The brain with the attached uppermost spinal cord was removed after the general autopsy using a bone saw with a vacuum attachment to minimize personnel exposure to bone dust. Tissue samples (up to ~3 cm in the greatest dimension) from the olfactory bulb/gyrus rectus, superior frontal gyrus, mesial temporal lobe with the anterior hippocampus and amygdala, cerebellum and medulla oblongata were placed in clean plastic bags, sealed, marked, frozen on dry ice and stored at –80°C in the Columbia University BioBank laboratory dedicated to storing and processing COVID-19 autopsy tissues. After removing tissue for freezing, each brain was fixed in 10% buffered formalin for 10 days. After brain removal, parallel longitudinal cuts were made in the medial anterior cranial fossa to circumferentially excise the cribriform plate of the ethmoid bones along with underlying olfactory and nasal epithelium. A small piece of nasal epithelial tissue was sampled for qRT-PCR, and the remainder divided for freezing and fixation in 10% formalin.

Tissue processing

After ~10 days in formalin fixation, brains were externally examined, the cerebral hemispheres were sliced in the coronal plane, the brainstem in the transverse plane and the cerebellum in the sagittal plane. An extensive set of tissue blocks were processed for paraffin embedding in cassettes, which included olfactory bulb/tracts with adjacent gyrus rectus, superior frontal cortex, striatum at the level of the globus pallidus, anterior thalamus, anterior hippocampus, hippocampal formation at the level of the lateral geniculate body, amygdala, striatum at the level of the nucleus accumbens, calcarine cortex, cerebellum with dentate nucleus, corpus callosum (genu), corpus callosum (body with cingulate cortex), corpus callosum (splenium), rostral midbrain, caudal midbrain, rostral pons, caudal pons, four sequential slices of the medulla, cervical spinal cord, pituitary gland, pineal gland, choroid plexus from the lateral ventricle, nasal epithelium and vessels of the circle of Willis. Additional blocks were obtained depending on gross pathology, such as infarcts or haemorrhages.

Tissue staining

Sections of paraffin blocks were cut at a thickness of 7 μm and stained with haematoxylin and eosin. As routine measures, immunostaining for CD3, CD68 and glial fibrillary acidic protein (GFAP) were performed on sections of olfactory bulb with adjacent gyrus rectus, temporal lobe with hippocampus, pons, medulla and cerebellum. Immunostaining for SARS-CoV-2 nucleocapsid (N) protein (Sino Biological©; Cat #40143-R001) was performed on sections of nasal epithelium, olfactory bulb and medulla. Other sections were stained with these antibodies when appropriate. Immunostaining for the majority of cases was conducted in the Department of Pathology Immunohistochemistry Core Laboratory using routine protocols with the Leica™ Bond autostainer. All antibodies used are available for clinical diagnostics, including herpes simplex virus type 1 (HSV-1, Cell Marque #361 A-ASR).

In a subset of cases, additional immunoperoxidase staining was performed on paraffin sections of the pons and choroid plexus from the lateral ventricle, as described.[30] Sequential sections were immunostained for claudin 5 (CLDN5) (ThermoScientific 1:200), CD3 (Novus Biological, 1:100), CD31 (Dako, 1:50), CD68 (Novus Biologicals, 1:200), IBA1 (Wako, 1:250), collagen IV (Abcam, 1:300), laminin (Sigma; 1:60), vascular cell adhesion molecule-1 (VCAM1) (Abcam; 1:250) and zona occludens-1 (ZO-1) (ThermoScientific 1:200). Images were acquired with a Zeiss Axioimager using a colour camera and 10× or 20× objective.

Tissue analysis

Each brain was examined by at least two board-certified neuropathologists, and the key pathological findings were reviewed and discussed at a divisional conference (which includes eight board-certified neuropathologists). The findings reflect the consensus of our group.

Detection of SARS-CoV-2 by qRT-PCR in brain autopsy tissues

Quantitative RT-PCR was performed on 125 brain tissue samples from 25 autopsy cases. Samples were taken from different anatomic locations including the nasal epithelium ($n = 21$), olfactory bulb ($n = 25$), superior frontal gyrus ($n = 7$), temporal lobe ($n = 25$), cerebellum ($n = 23$) and medulla oblongata ($n = 24$). The samples were obtained from either fresh or frozen sections and immediately placed in DNA/RNA shield (ZYMO Research; Cat# R1200-25). RNA was extracted using an RNeasy® Mini Kit (Qiagen) and qRT-PCR was performed using TaqMan™ 4× master mix using SARS-CoV-2 primer/probe sets (IDT) against the N region to detect the presence of virus per CDC recommendations [2019 Novel Coronavirus Real-Time Reverse Transcriptase (RT)-PCR Diagnostic Panel]. Each assay included a standard curve to determine the viral load (log10 copies/sample).

Detection of SARS-CoV-2 by RNAscope® in brain autopsy tissues

RNAscope® was performed on 21 fresh frozen brain samples. These were from the medulla ($n = 16$), four olfactory bulbs and one cerebellum. For positive controls we used three lung specimens from patients that had high SARS-CoV-2 viral loads [cycle threshold (Ct) values from 18 to 19 for the N region]. Five ready-to-use probes were acquired commercially: an antisense probe for the *N* gene of SARS-CoV2 (#846081; cross-reacts with SARS and MERS), an antisense probe for the spike (*S*) gene of SARS-CoV-2 (#848561; unique to SARS-CoV2), a negative control antisense probe for the *LAT* gene of HSV-1 (#315651), a negative control antisense probe for the *dapB* gene of *Bacillus subtilis* strain SMY (#310043) and a positive control antisense probe for the human *CLDN5* gene (#517141; a vascular marker) [ACD Biotechne (ACD)]. Probes were composed of 20–40 ZZ oligo-probes, except the *dapB* probe, which was composed of 10 ZZ oligo probes; the sequences of probes are proprietary. RNAscope® was performed using a 2.5 HD Red Detection Kit according to the manufacturer's recommendations (ACD). Briefly, fresh frozen sections were fixed in 4% paraformaldehyde for 10–15 min, washed 3× with phosphate-buffered saline (PBS) for 5 min each wash and dehydrated in graded ethanol series (50%, 70% and 100% ethanol) for 5 min. Slides were processed immediately or

stored in 100% ethanol at –20°C for up to 1 week. Slides were dried for 5–10 min at room temperature, pretreated with 3% hydrogen peroxide for 10 min and protease IV for 15 min (ACD) and incubated with probe solution for 2 h at 40°C in the HybEZ™ oven (ACD). *In situ* hybridization (ISH) signal was amplified following the manufacturer's recommendation, except that AMP5 incubation was increased to 45 min. Slides were developed in WarpRed chromogen (Biocare Medical) for 10–15 min at room temperature, counterstained with haematoxylin (Gill II formulation, Ricca Chemical Company) and mounted with Permount™ (Sigma Aldrich). Images were acquired with a Zeiss Axioimager using a colour camera and 20× objective. RNA ISH was also performed in the Department of Pathology clinical laboratory as previously described using two probes to the SARS-CoV-2 RNA encoding the spike protein.[31]

Data availability

All data are available upon reasonable request.

Results

Clinical data

The patients' mean age was 74 years (range 38–97); 27 patients (66%) were male and 24 (83%) were of Hispanic/Latinx ethnicity. The most frequent presenting symptoms included dyspnoea (27/41; 66%), cough (18/41; 44%) and confusion (13/41; 34%) (Supplementary Tables 2 and 3). The average time from symptom onset to hospital presentation was 6 days (range 0–12 days), and the average length of hospitalization was 19 days (range 0–69 days) (Fig. 1). Three (7%) patients presented in acute cardiopulmonary

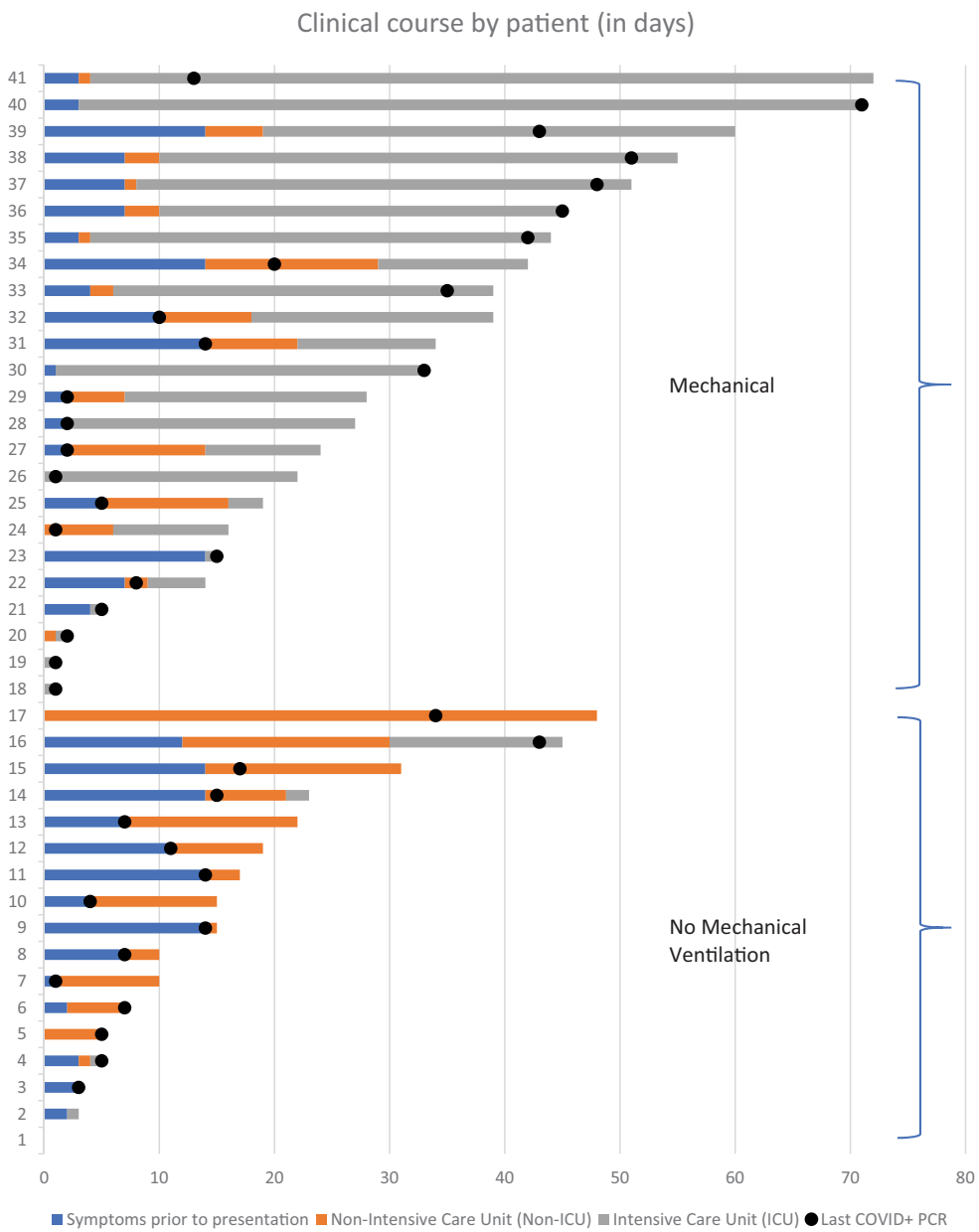

Figure 1 Clinical course of COVID-19 patients by days. Bar graph showing the length of the clinical course of our patients, including symptoms prior to presentation (blue) and days in the hospital before death, either in the intensive care unit (grey) or not in the intensive care unit (orange). Dots represent the last positive qRT-PCR result prior to death. Patients are numbered 1–41 and displayed from shortest to longest clinical course.

distress with rapid progression to death. Dementia or mild cognitive impairment was the most common neurological comorbidity (8/41; 20%), identified by review of electronic medical records. Chest X-rays on admission showed multifocal pneumonia in 33 (81%) of patients. Twenty-four patients (59%) were admitted to the intensive care unit. Hospital-associated complications were common, including deep-vein thrombosis/pulmonary embolism in eight (20%) patients, acute renal failure requiring dialysis in seven (17%) and bacteraemia in 10 (24%). Seven (17%) patients had a neurology consult during their hospital admission, and one was admitted to the stroke service. Eight (20%) patients died less than 24 h after hospital admission, seven (17%) in less than 1 week, 15 (37%) in 1–4 weeks and 11 (27%) over 4 weeks after hospital admission (Fig. 1). The average time between death and autopsy was 26 h (range 2–177 h); 31/41 (76%) of the autopsies were performed within 24 h. The majority of patients for whom laboratory testing was performed showed elevated inflammatory markers. In the 30 patients with C-reactive protein measurements; 12 (40%) patients had peak values over 300 mg/l and 18 (60%) had an average of 186.2 (range 12.9–285.2). Peak interleukin (IL)-6 levels were markedly elevated in 26 (96%) of the 27 patients tested (Supplementary Table 4).

Ante-mortem and post-mortem neuroimaging

Head CTs were performed on 11 (27%) patients during their hospital stays and two (5%) also underwent a brain MRI (Supplementary Table 2). Parenchymal haemorrhages/haemorrhagic infarcts were identified in three patients and multiple cortical and deep grey nuclei early subacute infarcts in one patient. Five patients had diffuse cerebral oedema and hypoxaemic injury, three of whom exhibited concurrent or prior haemorrhages, and one of these also showed bilateral basal ganglionic petechial haemorrhages. Nine brains (22%) were imaged post-mortem: one brain with multiple cortical haemorrhagic infarcts and a right basal ganglionic infarct, one with mild cortical haemorrhage, one with minimal bilateral basal ganglionic haemorrhages, one with a right occipital parenchymal haemorrhage and two with intraventricular haemorrhages. An example of premortem, post-mortem and corresponding neuropathology of acute haemorrhagic infarcts is shown in Fig. 2.

Neuropathological findings

Hypoxic/ischaemic injury was the most common pathology

All brains contained hypoxic damage, varying from acute to subacute. Acute changes included neuronal shrinkage and eosinophilia with or without neuronal loss, reactive astrocytosis, highlighted with GFAP immunostaining, and subacute hypoxic changes manifested as subacute infarcts with variable macrophage infiltrates, reactive astrocytosis and neovascularization. These findings were widespread in most brains, but in a few patients (9/41; 22%) were more focal, predominantly involving the isocortex, hippocampus, cerebellum and/or brainstem (Table 1).

Vascular pathology was also common

Eighteen (44%) brains contained infarcts, acute, subacute, or chronic in isocortex, striatum, thalamus, hippocampus, corpus callosum and brainstem, with 10 (24%) containing one or multiple small infarcts (Table 1). None of the larger infarcts appeared to represent watershed infarcts. Eight (19%) brains contained haemorrhages involving isocortex, white matter, cerebellum, brainstem and/or the subarachnoid space. These ranged from multifocal, perivenular haemorrhages, to large haemorrhages, the largest in the cerebellum. The majority of haemorrhages appeared to represent ischaemic infarcts that became haemorrhagic, evidenced by small haemorrhages adjacent to infarcted tissue (Fig. 2A–H).

The majority of brains (36/41; 88%) showed atherosclerotic changes in the circle of Willis and arteriolosclerosis in smaller intraparenchymal arteries and arterioles. We did not detect vasculitis, defined as fibrinoid necrosis of vessel walls or the destruction of vessels walls with intramural inflammatory cells.

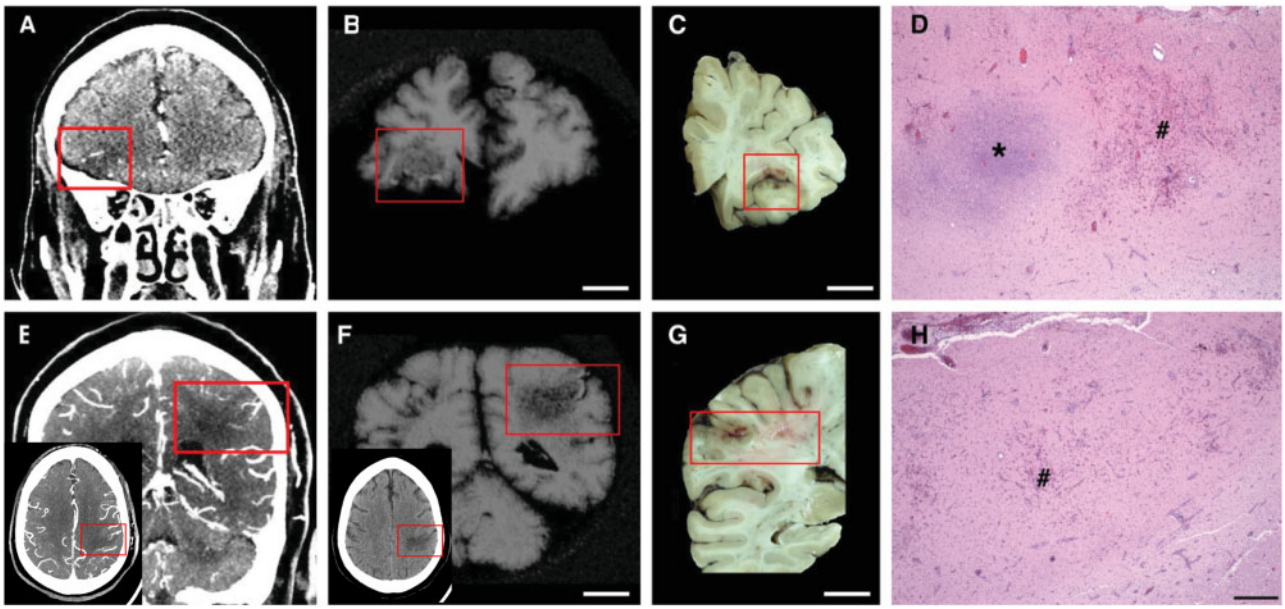

Figure 2 Acute, focal, haemorrhagic infarcts in COVID-19 patients. Acute, focal, haemorrhagic infarcts of (**A**–**D**) right inferior frontal and (**E**–**H**) left lateral parietal lobes. (**A** and **E**) Premortem CAT scans; (**B** and **F**) post-mortem MRI; (**C** and **D**) gross photographs of coronal brain slices through the corresponding infarcts; and (**D** and **H**) microscopic images of the corresponding infarcts. The *insets* in **E** and **F** show the parietal infarct in the axial plane, red boxes outline the lesions on the scans and brain slices. (**D** and **H**) Areas of fresh haemorrhage (number symbol) and acute necrosis (asterisk) shown with haemoxylin and eosin stain. Scale bar in **H** = 500 μm for **D** and **H**; **B**, **C**, **F** and **G** = 1 cm.

Table 1 Neuropathology findings

Neuropathology	*n*/Total (%)
Hypoxia	41/41 (100) focal to global
Infarcts[a]	18/41 (43.9)
Haemorrhage	8/41 (19.5)
Lymphocytic infiltrates	38/41 (92.6) mild
Microglial activation, focal or diffuse	34/41 (80.5)
Microglial nodules/neuronophagia	26/41 (63.4)
Acute thrombosis	3/41 (7.3)
Athero- arteriolo-sclerosis	36/41 (87.8) mild to severe
AD, CAA, PD, PSP, PART pathology	18/41 (43.9)
Herpes encephalitis	1/41 (2.4)

For the cases with Alzheimer's and Lewy body pathology, the median and range of Braak neurofibrillary tangle score and the Lewy body disease type was assessed. Using the NIA 'A, B, C' Alzheimer's disease pathology score,[32] we observed the following: brains with Alzheimer's disease pathologies ranged from A0–A5 with a mean of 43/19 = 2.26 and median of 2; B0–B6 with a mean of 64/19 = 3.34 and median of 3; C0 (10), C sparse (2), C moderate (4), C severe (1). Lewy body disease type: brainstem (3), cortical (2). AD = Alzheimer's disease; CAA = cerebral amyloid angiopathy; PD = Parkinson's disease; PSP-progressive supranuclear palsy; PART = primary age-related tauopathy.

[a]Infarcts: six brains with chronic infarcts, 12 with acute or subacute infarcts; seven with microscopic acute or subacute infarcts (not seen grossly); nine with multiple infarcts, one of them with chronic infarcts; locations: isocortex (*n* = 9), corpus callosum (*n* = 5), pons (*n* = 5), midbrain (*n* = 1), thalamus (*n* = 2), caudate (*n* = 1), putamen (*n* = 1), hippocampus (*n* = 2, both chronic) and pituitary (*n* = 2).

Immunostaining for the vascular basement membrane proteins such as Collagen IV and Laminin or the tight junction proteinZO-1 showed intact capillary and venular walls (Supplementary Fig. 1A–F). One patient, who had disseminated HSV-1 infection with CNS involvement (see below), showed a clear loss of vascular basement membrane proteins and ZO-1 immunostaining (Supplementary Fig. 1G–I) and an increase in VCAM1 (data not shown).

Microglial activation was present in the majority of COVID-19 brains

We defined microglial activation by enlargement of cell soma and thickening of processes detected by either IBA1 or CD68 immunostaining. Diffuse microglial activation was present in the majority of the brains (34/41; 81%), variably involving many brain areas (Table 1). Microglia also appeared in clusters (microglial nodules) in over half of the brains (26/41; 63%). Small clusters of $CD3^+/CD8^+$ T cells were associated with prominent microglial nodules in a few cases (Fig. 3C, D and Supplementary Fig. 2A, B, E and F). Neurons were present in some of these microglial clusters (Fig. 3A, B, E–I and Supplementary Fig. 2A, B, E and F), representing neuronophagia. The microglial nodules were most prevalent in the brainstem, where they appeared particularly common in the inferior olivary nucleus and the tegmental nuclei of the medulla and pons, including the locus coeruleus, hypoglossal nucleus, dorsal vagal motor nucleus, solitary nucleus and midline raphe (Fig. 3A–G and Supplementary Fig. 2A–F). They were also present in the cerebellar deep nuclei (Fig. 3H and I) and white matter, although not in the cerebellar cortex, except one patient who had concomitant HSV-1 encephalitis and diffuse microglial activation (Supplementary Fig. 2I and J). The microglial nodules were less frequent in the hippocampus (8/41; 20%), where they preferentially localized to the pyramidal cell layer (Fig. 3J and K) and in the isocortex (2/41; 5%) and olfactory bulb (2/41; 5%).

Perivascular lymphocytic inflammation and infiltration into the brain parenchyma was sparse

In 38 (93%) brains, we found scant lymphocytic infiltration, predominantly around blood vessels, with very few $CD3^+$ T lymphocytes penetrating into the brain parenchyma and meninges (Figs 3C, D and 4A and C). Immunostaining for CD20 revealed no B lymphocyte infiltration (data not shown). One brain showed very large perivascular and intraparenchymal T cell and macrophage infiltrates concomitant with an HSV-1 infection (Fig. 4E and Supplementary Fig. 2I and J), providing a stark contrast to the modest level of lymphocytic infiltration seen in COVID-19 brains. We also observed few lymphocytes in the choroid plexuses from lateral ventricles of 16 brains, except one with HSV-1 encephalitis that contained prominent T cells and activated microglia (Fig. 4B, D, F and Supplementary Figs 2K, L and 5D–F). Consistent with sparse immune cell infiltrations in the CNS of COVID-19 cases, we also found that expression of tight junction proteins in the choroid plexus epithelial cells was intact with the exception of the HSV-1 encephalitis case, where tight junction staining was completely lost (Supplementary Fig. 3).

Many patients showed the pathology of neurodegenerative diseases

Given the ages of our patients and the ante-mortem histories of dementia/mild cognitive impairment and Parkinson's disease in some patients (Table 1), it was not unexpected that 19 brains contained neurofibrillary tangles, with and without amyloid plaques (17/41, 41.4%) and Lewy bodies of Parkinson's disease (3/41, 7%). One of these 18 patients had both Alzheimer's and Parkinson's pathology. Of note, only eight had an ante-mortem diagnosis of dementia/mild cognitive impairment and three a history of Parkinson's disease.

Demyelination was not evident

Because of a report of acute disseminated encephalomyelitis-like pathology in a COVID-19 patient,[24] we examined all brains for demyelination but did not find evidence of it. While we cannot rule out the possibility that some of the areas of brains that were not sampled contained foci of demyelination, we note that brains were extensively sampled in 20–30 regions for histopathology.

Multifocal necrotizing leukoencephalopathy in one patient

We found lesions consistent with multifocal necrotizing leukoencephalopathy in the pons in one patient, showing small foci of necrosis, myelin loss, oedema and axonal swellings (Supplementary Fig. 4). This 74-year-old female with hypertension and hypothyroidism was admitted after 1 week of fever, cough and chills in hypoxaemic respiratory failure. She developed acute kidney injury requiring renal replacement therapy, severe hypoxaemia requiring paralysis and pronation and multiple other infections (*Escherichia coli* urinary tract infection, methicillin-susceptible *Staphylococcus aureus* pneumonia and recurrent candidiasis in respiratory and urine cultures). The patient's status acutely worsened with septic shock in the context of *Pseudomonas aeruginosa* ventilator-associated pneumonia and bacteraemia.

Pathology in the olfactory bulbs was mild

Because of widespread speculation that SARS-CoV-2 may enter the brain via the olfactory route,[33] we examined olfactory bulbs in all patients. We found variable, albeit generally sparse numbers of T cells in the parenchyma, mild-to-moderate patchy microglial activation and very few microglial nodules, indicating no major histopathology in this region (data not shown).

One brain contained HSV-1 encephalitis

One of our patients also had a disseminated HSV-1 infection with CNS involvement, diagnosed only post-mortem (Patient 22). This 70-year-old female with hypertension, living independently, developed acute

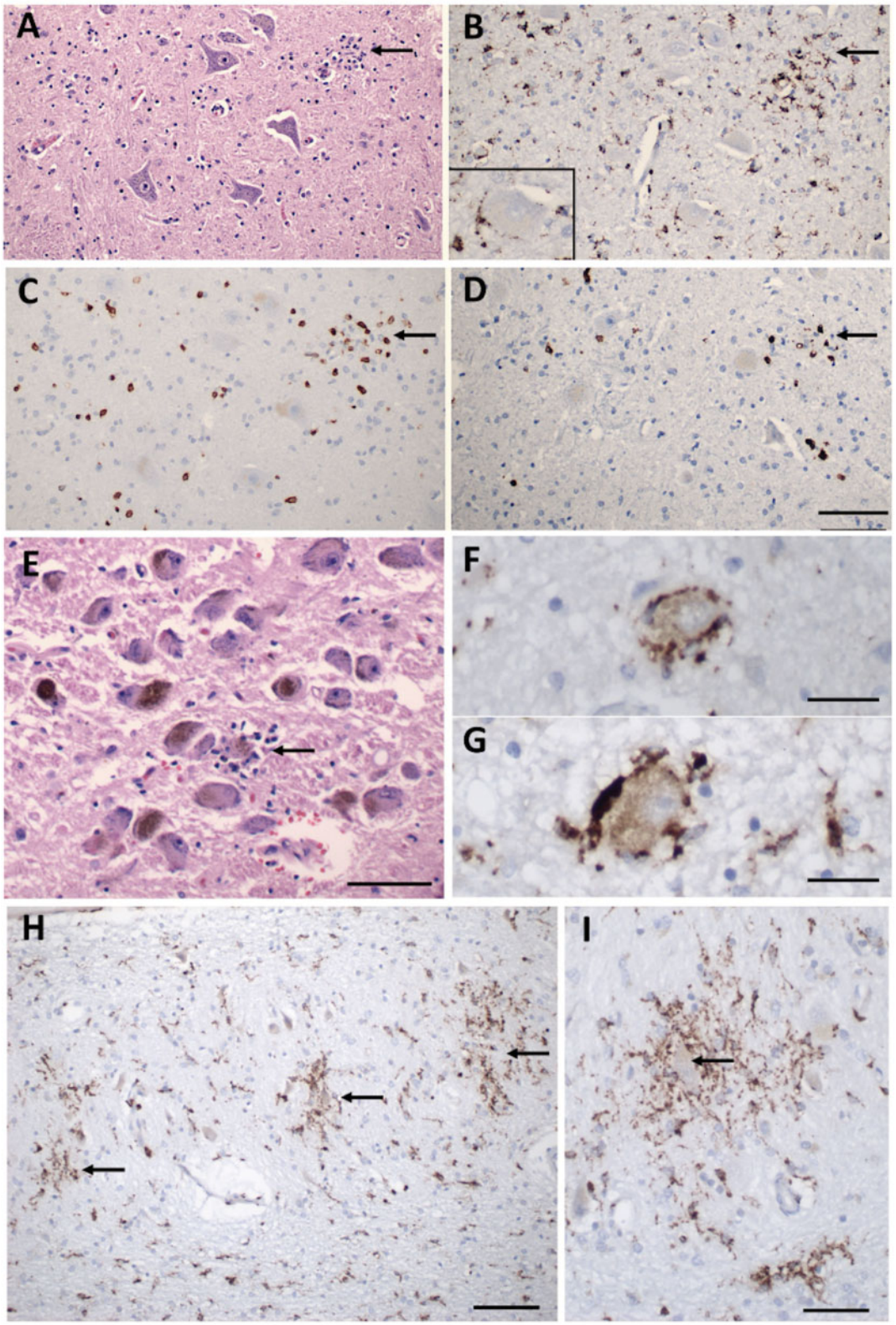

Figure 3 Inflammatory pathology in COVID-19 brains. (**A**) Section of the hypoglossal nucleus shows several motor neurons and a microglial module (arrow). (**B**) An adjacent section stained for CD68, showing clustered microglia in the nodule. *Inset*: Microglia in close apposition to a hypoglossal neuron (CD68). (**C**) An adjacent section stained for CD3, showing scattered T cells in the tissue and associated with the microglial nodule. (**D**) An adjacent section stained for CD8 showing that many of the T cells are $CD8^+$. (**E**) The locus coeruleus contains a microglial nodule with a degenerating neuron in the centre, identified by its residual neuromelanin (arrow). (**F** and **G**) Neurons of the dorsal motor nucleus of the vagus surrounded by $CD68^+$ microglia. (**H** and **I**) Microglial nodules in the dentate nucleus (arrows in **H**), neuron in the middle of a nodule (arrow in **I**), CD68. Scale bar in **D** = 200 μm for **A**–**D**; in **E** = 10 μm; **F** and **G** = 50 μm; **H** = 100 μm; **I** = 50 μm; **J** = 1 mm; and **K** = 250 μm.

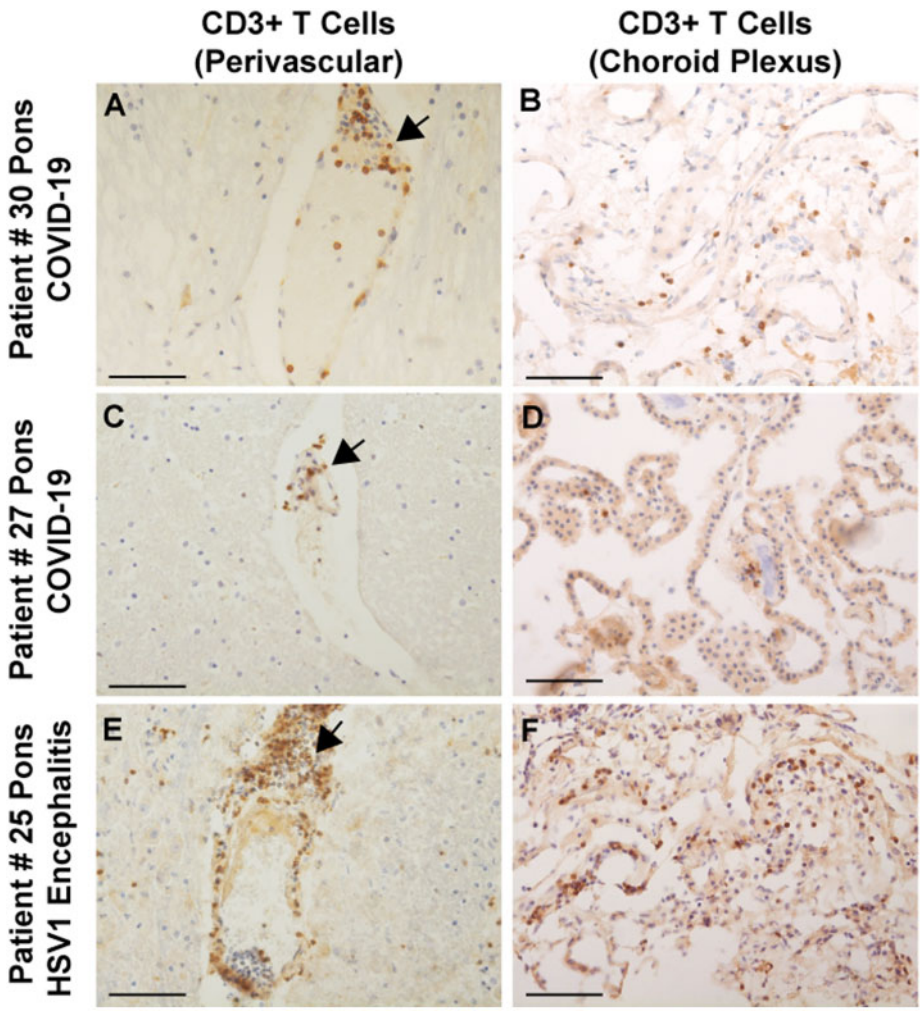

Figure 4 Immunocytochemical staining for CD3$^+$ T cells in COVID-19 brains. (**A** and **C**) Sparse perivascular CD3$^+$ T cells in the pons of COVID-19 Patients 27 and 30. (**B** and **D**) Sparse CD3$^+$ T cells in the choroid plexus from the lateral ventricle of Patients 27 and 30. (**E** and **F**) CD3+ T cell infiltrates around a pontine vessel (**E**) and in the choroid plexus (**F**) of Patient 25 with HSV-1 encephalitis; arrows indicate CD3$^+$ T cell infiltrates. All sections are counterstained with haematoxylin. Scale bars = 200 μm.

respiratory distress and vasodilatory shock in the context of COVID-19. She developed acute renal failure, *Staphylococcus epidermidis* bacteraemia, *P. aeruginosa* ventilator-associated pneumonia and cytomegalovirus viraemia during her prolonged hospitalization. Because of her refractory hypoxaemia after 44 days of hospitalization, she was palliatively extubated and died within minutes. We found disseminated HSV-1 infection with CNS involvement, proven by immunocytochemistry (Supplementary Fig. 5C). In contrast to COVID-19 neuropathology, the brain had prominent lymphocytic infiltrates in the parenchyma, meninges, and choroid plexus, vasculitis, severe microglial activation and microglial nodules (Fig. 4E, F and Supplementary Figs 1G–I, 2I–J and 5). In addition, there was a reduction or loss of collagen IV and laminin in the basement membrane of blood vessels, loss of ZO-1 expression in endothelial cells in proximity to massive T cell infiltrates (Supplementary Fig. 1G–I) and loss of CLDN5 expression in the epithelial barrier of the choroid plexus (Supplementary Fig. 3D and D').

Molecular findings

Quantitative RT-PCR detected very low levels of viral RNA in some brains

To determine whether SARS-CoV-2 was present in the brain, we conducted qRT-PCR for the *N* gene in four different brain areas in the first 25 patients of this series. We also examined the nasal epithelium for most of these patients as an internal control. Nearly all available nasal epithelium samples (19/21; 91%) were highly positive for SARS-CoV-2 according to the qRT-PCR analysis. The median viral copy/sample for nasal epithelium was 43 840 (Supplementary Table 5). For CNS samples, the proportion of positive samples as well as the number of viral copies was significantly lower (Fig. 5 and Supplementary Table 5). In 7/25 (28%) patients, all CNS sites were negative for SARS-CoV-2, whereas 18/25 (72%) patients had at least one very low but positive CNS site and 9/25 (36%) patients had multiple very low but positive CNS sites (Fig. 5). The cerebellum was most commonly positive (10/23; 44%), followed by samples from the olfactory bulb (10/25; 40%), the temporal lobe (9/25; 36%) and the medulla (8/24; 33%). We did not find any correlation between detection of viral RNA by qRT-PCR and the histopathological findings discussed above. For example, no microglial nodules were seen in any of the olfactory bulb samples that were analysed by qRT-PCR (0/25), whereas the medulla samples showed prominent microglial activation, with the majority of samples analysed by qRT-PCR containing microglia nodules (14/24), yet there was no significant difference in the viral levels detected in olfactory bulb samples compared to medulla samples (paired sample *t*-test: $P = 0.309$). Furthermore, we compared the

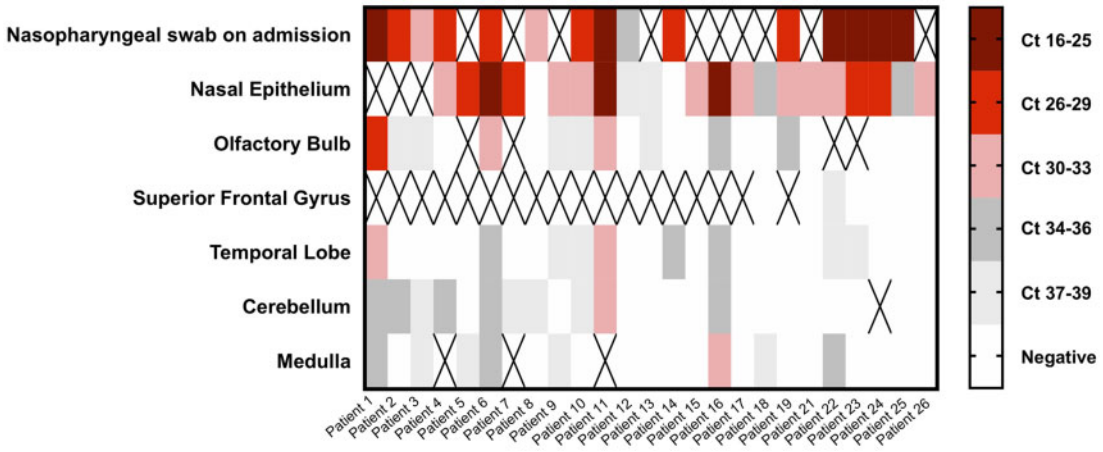

Figure 5 SARS-CoV-2 qRT-PCR results from the nasal epithelia and brains of COVID-19 patients. Heat map of cycle threshold (Ct) values of brain autopsy sample qRT-PCR for detection of SARS-CoV-2. Nasopharyngeal swab at the time of admission and nasal epithelium are included as samples outside of the CNS. Ct values are presented in quintiles based on the distribution in samples tested. 'X' denotes sample not included for that patient.

viral levels in medulla samples with microglial nodules to those without microglial nodules, and again found no significant difference (Mann Whitney U-test: $P = 0.710$, independent sample *t*-test: $P = 0.770$).

SARS-CoV-2 mRNA was not detected in brain tissue by RNAscope®

The presence of low levels of viral RNA in at least one brain region in 18/25 (72%) COVID-19 patients raised the question as to whether the virus is present in the brain or associated with the vasculature or blood components, including infiltrating macrophages. We performed RNAscope® on fresh frozen COVID-19 brain sections for 16 cases, including sections from the medulla ($n = 16$), olfactory bulb ($n = 3$) and cerebellum ($n = 1$) (Supplementary Table 6). The brains were selected based on qRT-PCR data to include areas that were either high, low positive, or negative for the viral RNA by RT-PCR. Lung sections from three COVID-19-positive cases in a different series that had high CT values (18-19 for the *N* gene) according to RT-PCR were selected as positive controls for the RNA scope. In contrast to the RT-PCR data, we could not detect viral RNA on fresh frozen brain sections using either an antisense probe for the S or N region, or a combination of both probes in cases that were either positive or low positive by RT-PCR (Fig. 6A, B and D–G). However, we could detect abundant RNA for SARS-CoV-2 S or the N region in the COVID-19 lung sections (Fig. 6C, F and I). As a positive control for brain sections, we detected *CLDN5* mRNA (an endothelial cell marker) in medullas (Fig. 6J). Notably, in one case (Patient 18), we detected viral RNA for the S region in perivascular cells in the adventitia of a large blood vessel outside the medulla, suggesting sporadic infection of blood vessel cells (Fig. 6K). Overall, our findings suggest that if SARS-CoV-2 is present in brain tissue, either its levels are very low and below the limits of detection by RNAscope®, or the virus had already been cleared in some brains.

Immunohistochemistry did not detect viral proteins in COVID-19 brains

We performed immunocytochemistry for SARS-CoV-2 N protein on sections of olfactory bulb and medulla on all brains. Other sections of brains were stained when appropriate, such as those that showed high numbers of microglial nodules or infarcts. All brain sections showed no staining; however, the nasal epithelium was positive (Supplementary Fig. 6). N protein antibody staining of lung tissues of some of our patients also stained positively (data not shown).

Discussion

Gaps in our understanding of SARS-CoV-2 infection remain. There is a paucity of detailed neuropathological data, critical to understanding the neuro-invasive capacity of SARS-CoV-2 and mechanisms of neurological injury. In this retrospective study of 41 patients, we provide detailed investigations of the clinicopathological and molecular characteristics of COVID-19 in post-mortem brain samples. Strengths of our study include the multi-ethnic group of patients, detailed clinicopathologicalstudies, the wide spectrum of hospital courses from less than 1 day to many weeks and a multi-pronged effort to detect viral RNA and protein in the brains in conjunction with histopathology. Many of the pathological changes can be attributed to the effects of hypoxia, coagulopathy and multi-organ damage in severe infection, accompanied by virus-mediated inflammatory processes such as systemic cytokine release, while other changes reflect the age range and comorbidities of our patients.

RNAscope® and immunocytochemistry did not detect viral RNA and protein in the brains

Quantitative RT-PCR analyses of nasal epithelium and brain tissues provide evidence for the presence of viral RNA, albeit at very low levels in the brain. The high positive levels in the nasal epithelium were unexpected in some patients, given that nine patients were sampled, at the time of autopsy, more than 1 month after their initial diagnosis by nasal pharyngeal swabs. While several RT-PCR studies have suggested prolonged shedding in some patients,[34,35] our findings indicate that either individuals who died have prolonged viral or that viral persistence in the nasal epithelium can last even longer than previously anticipated.

We detected low viral loads of SARS-CoV-2 in at least one CNS section from a substantial proportion of patients. While there is some variation among sites, the relatively low levels of viral RNA suggest that there is poor CNS tropism of SARS-CoV-2, compared with SARS or MERS. The low viral load is in concordance with recent studies,[28,33,36] which report low viral loads in some, but not all of the

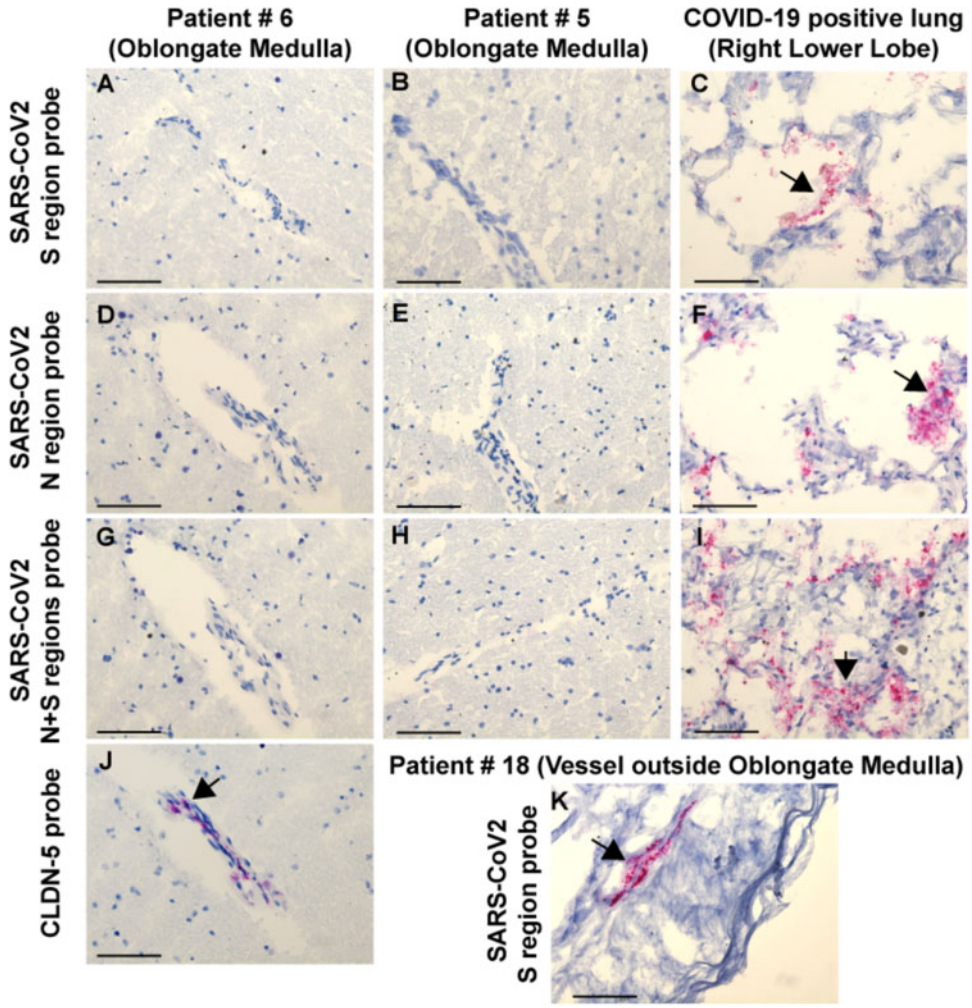

Figure 6 RNAscope® results from the brains and lungs of COVID-19 patients. RNAscope® with SARS-CoV-2 S region probe on (**A**) medulla Patient 6, (**B**) medulla Patient 5, and (**C**) lung, positive control. SARS-CoV-2 N region probe on (**D**) medulla Patient 6, (**E**) medulla Patient 5, and (**F**) lung, positive control. SARS-CoV-2 N + S region probes on (**G**) medulla Patient 6, (**H**) medulla Patient 5, and (**I**) lung, positive control. (**J**) *CLDN5* probe on medulla Patient 6 showing a positive signal in endothelial cells. (**K**) SARS-CoV-2 S region probe gives a positive signal in the adventitia of a meningeal vessel outside of medulla Patient 18. All sections were counterstained with haematoxylin. Arrows indicate positive RNAscope® signal. Scale bars = 200 μm.

brain sections tested by RT-PCR. Convincing microscopic evidence of virus in the brain is lacking in our study, since RNAscope® and immunohistochemistry failed to identify viral RNA or protein for the N or S regions in the brain or choroid plexus. Quantitative RT-PCR may be more sensitive, since our RNAscope® detected viral RNA in lungs that had Ct values of 18–19 for the *N* gene (data not shown). However, a possible source of SARS-CoV-2 in brain tissues is haematogenous viral RNA within CNS blood vessels or haemorrhages, as we demonstrated in a recent case report on one of our patients (Patient 10).[37] It is also possible the viral RNA in some leptomeningeal vessels, as seen by RNAscope® (Fig. 6K), contributes to the low levels of virus seen by RT-PCR in some tissue samples. Furthermore, viral contamination during the different stages of the autopsy cannot be excluded. However, the nasal epithelium and the CNS sections were obtained during different autopsy procedures, making it unlikely that contamination from the nasal epithelium contributed to positive qRT-PCR findings. Moreover, appropriate negative controls were included in qRT-PCR assays, and repeat qRT-PCR of select sections confirmed their positive and negative status.

We interpret these very low levels of SARS-CoV-2 seen in some samples with caution. While we cannot completely exclude the possibility that viral protein or RNA is present in these brains, our observations indicate that if there, the levels must be extremely low, supporting our conclusion that the neuropathological findings are unlikely to be caused by viral infection of brain tissue. Furthermore, we found no correlations between qRT-PCR results in medullary sections and the presence of microglial activation and microglial nodules, since medullas that tested negative by qRT-PCR still contained activated microglia. Several studies have also failed to detect viral proteins by immunostaining.[28,38,39] Rare positive cells of undefined nature have been reported.[40] Further studies examining CSF or brain from newly infected individuals or the use of double-stranded RNA probes to identify remnants of replicating virus may help determine any neurotropism for SARS-CoV-2.

Microglial activation is widespread, but most common in the brainstem

A large majority of brains had prominent microglial activation in multiple areas. As expected, activation often corresponded to areas containing hypoxic damage or infarcts. However, we observed many areas of focal microglial activation characterized by microglial nodules, many of which contained neurons. These were most prevalent in the lower brainstem, although more rarely

in other areas. In the medulla, both the inferior olivary nucleus and a number of tegmental nuclei were involved. Microglial nodules are characteristically present in viral and autoimmune encephalitis, in which neurons contain viral antigens or autoimmune antigens,[41] and in animal models of recovery from neurotropic viruses such as Zika virus, neuronophagia is observed in brain regions with demonstrated viral targeting.[42] Despite the presence of microglial nodules and neuronophagia, we were unable to detect viral RNA or protein in these areas. Thus, it seems likely that interactions between microglia and neurons were not a direct response to viral infection of neurons but rather were secondary to hypoxic/ischaemic injury in the setting of a systemic inflammatory process.

All patients suffered some degree of hypoxia, a condition known to produce signals in neurons that attract and activate microglia,[43] leading to phagocytosis. Microglial nodules are not commonly associated with diffuse or focal hypoxic damage, although our findings suggest that hypoxia may contribute to this type of microglial activation, particularly in the setting of a systemic inflammatory process. Furthermore, microglial activation accompanies sepsis.[44] Although a minority of our patients were known to be bacteraemic, others may have met criteria for septic shock and were receiving antibiotics. A careful review of the brains of patients with acute respiratory distress syndrome, prolonged coma, associated bacteraemia and hypoxia in pre-COVID years would be important future efforts.

An immunological cause of activated microglia and neuronophagia is a further consideration, perhaps made worse by hypoxia. The smaller microglial nodules had little or no T cell component, while larger ones included some T cells. Such pathology could represent a spectrum of inflammatory development as postulated in Rasmussen's encephalitis,[45] a model in which microglia first attacked neurons and secondarily attracted T cells, or T cell-mediated microglial activation and phagocytosis, as shown in flavivirus infections.[42] Otherwise, we found little T cell presence in the parenchyma, perivascular areas, meninges or choroid plexus. Notably, with the exception of the one patient who had HSV-1 encephalitis, none of the COVID autopsy brains showed histopathological features of limbic encephalitis. Furthermore, considering the sparse lymphocytic infiltrate, the histopathological findings were not suggestive of autoimmune encephalitis.

Neuronal damage and loss in the lower brainstem could cause a number of clinical features, including altered cardiac and respiratory regulation, cranial nerve motor findings, somnolence, insomnia and other signs and symptoms. It was unlikely that these were discovered in such ill patients, many of whom were heavily sedated on ventilatory support. The reason for a predominant brainstem localization of microglial nodules is not clear but has been described in other reports (Supplementary Table 1). The involvement of multiple brainstem areas and nuclei are characteristic of several infectious and autoimmune disorders.[46]

Infarcts are common

A number of our patients suffered acute or subacute infarcts, which were likely to have occurred during the course of the disease, and many of these were diagnosed post-mortem. The locations of infarcts did not conform to a stereotypic pattern, since many different areas were involved in different individuals. The small infarcts associated with haemorrhages were most consistent with thrombotic or thromboembolic events and reperfusion. However, we only observed thrombi in a small number of brains (3/41; 7%). Furthermore, we did not find vasculitis, defined either as fibrinoid destruction of vessel walls or inflammatory cells within vessel walls. Indeed, immunostaining for structural components of the vascular basement membrane revealed intact blood vessels.

Many patients have pathological comorbidities

Given the patients' mean age of 74, we were not surprised to see atherosclerosis and arteriolar sclerosis. These could have limited blood flow and oxygenation diffusely or focally in patients with respiratory or cardiac failure. Several brains contained cerebral amyloid angiopathy, but none was associated with haemorrhage. Some of the older patients had amyloid plaques and tau tangles and three brains contained Lewy bodies. These neurodegenerative pathologies must have preceded the SARS-CoV-2 infection, but whether or not they contributed to the acute and subacute pathologies is not clear.

Tissue sampling in space and time

We submitted 20–30 sections per brain, including many regions. We only sampled the upper cervical spinal cord, so any lower cord pathology remains uncharacterized. Thus, even sampling many areas, we could have failed to identify relevant, local pathologies in unsampled areas.

Our patients suffered a broad time range of illness, from expiration on arrival at the hospital up to several months in the hospital (Fig. 1). However, we found similar neuropathology marked by prominent microglial activation with microglial nodules and neuronophagia in patients with both short and lengthy courses. Furthermore, the fact that we did not see detectable levels of virus by RNAscope® or immunohistochemistry in any of these cases, and detected only very low levels of virus by qRT-PCR, argues against the possibility that we have systematically missed some time point or location at which there is abundant virus after which the virus might be cleared from the brain.

Our findings may have implications for COVID-19 survivors

It is important to consider the potential impact of the neuropathological changes we, and others, have found in autopsies if such changes are present in the brains of patients who survive COVID-19. In light of the brainstem and hippocampal distribution of microglial activation, the latter of which has been linked to virus-induced cognitive deficits,[47] it is notable that some COVID-19 survivors develop neuropsychiatric symptoms, including memory disturbances, somnolence, fatigue and insomnia, and that similar symptoms are reported in both the acute and recovery phases. Critical to future work is understanding the short- and long-term consequences in survivors. This study included only patients who were severely ill and died. These changes may not be seen in patients with mild illness, and understanding the roles of contributing factors such as inflammation, multi-organ damage and hypoxia will require further studies.

Since the initial submission of this study, there have been other papers published describing the neuropathological findings in COVID-19 brain autopsies.[48–50] By and large, the findings of these other recent publications are consistent with our findings, and support the conclusion that the neuropathological findings of COVID-19 are most likely related to the systemic infection and hypoxic/ischaemic CNS damage, rather than direct viral invasion.

Limitations

This study has several limitations. Our patients, a multi-ethnic group, drawn from a single centre in New York City, may not represent the general COVID-19 population. Autopsy studies over-

represent severe cases, and our findings may not be generalizable to less severe cases. There are currently limited data on the sensitivity and specificity of SARS-CoV-2 qRT-PCR in various tissues including brain, and positive qRT-PCR in the brain may be due to virions in the blood rather than brain tissue. Additionally, clinical data for this study were obtained through retrospective chart review and thus fully reliant on electronic medical records. Most patients had significant pre-existing comorbidities, which confound our ability to attribute our findings to COVID-19 infection. Future studies with appropriate controls are needed to delineate which neuropathological findings result from COVID-19 infection and treatment and are not caused by other processes.

Conclusions

In our single centre study of 41 consecutive autopsies of COVID-19 patients we found significant neuropathology in all brains, most commonly diffuse hypoxic/ischaemic damage, acute and subacute infarcts, both large and small, the latter often with a haemorrhagic component, and diffuse and focal microglial activation, including neuronophagia, predominantly localized to the brainstem. There was sparse T cell infiltration and no evidence for acute vascular wall damage. Quantitative RT-PCR on multiple frozen brain tissues of many brains showed low or absent levels of viral RNA. RNAscope® and immunohistochemistry for S and N proteins were negative. Although we cannot conclusively rule out the presence of viral RNA and protein in these brains, we conclude that it is unlikely that viral infection of brain tissue directly accounts for the pathological changes.

Second, our predominantly older, Hispanic population had multiple comorbidities, including those only identified in the post-mortem period. Patients died in a range of time periods, with prolonged hospital courses associated with a significant number of hospital related complications. Notably, neuropathological findings did not appear to correlate with time of hospitalization, further suggesting that pathology was not closely correlated with hospital interventions like medications or mechanical ventilation.

Acknowledgements

The authors are most grateful to the patients' families, who gave us consent to perform autopsies; to the many members of the autopsy staff, who performed their duties under the most difficult circumstances; to our many colleagues in the Departments of Neurology, Pathology and Cell Biology, Radiology, and Medicine, who gave their unqualified support to these studies; and to Kevin Doyle, MA and Dr Anjali Saqi for helpful discussions and guidance with lung samples, Dr Hanina Hibshoosh and members of the Columbia University Tissue BioBank, Dr Jean-Paul Vonsattel for his invaluable input on neuropathological diagnoses and Ms Trine Giaever for illustrations.

Funding

Encephalitis and COVID-19 Seed Funding Award provided by the Encephalitis Society (E.H.M.) NS106014, supplement (J.C.) NIH/NINDS 1K23NS105935-01 (K.T.T.) Generous gift from Dr Yechiam Yemini (S.P.) Role of the funding source: the funder of the study had no role in study design, data collection, data analysis, data interpretation, or writing of the report. The corresponding author had full access to all the data in the study and had final responsibility for the decision to submit for publication.

Competing interests

The authors report no competing interests.

Supplementary material

Supplementary material is available at *Brain* online.

References

1. Nath A. Neurologic complications of coronavirus infections. *Neurology*. 2020;94(19):809–810.
2. Dugue R, Cay-Martínez KC, Thakur K, et al. Neurologic manifestations in an infant with COVID-19. *Neurology*. 2020;94(24):1100–1102.
3. Moriguchi T, Harii N, Goto J, et al. A first case of meningitis/encephalitis associated with SARS-Coronavirus-2. *Int J Infect Dis*. 2020;94:55–58.
4. Avula A, Nalleballe K, Narula N, et al. COVID-19 presenting as stroke. *Brain Behav Immun*. 2020;87:115–119.
5. Beyrouti R, Adams ME, Benjamin L, et al. Characteristics of ischaemic stroke associated with COVID-19. *J Neurol Neurosurg Psychiatry*. 2020;91(8):889–891.
6. Helms J, Kremer S, Merdji H, et al. Neurologic features in severe SARS-CoV-2 infection. *N Engl J Med*. 2020;382(23):2268–2270.
7. Mao L, Jin H, Wang M, et al. Neurologic manifestations of hospitalized patients with coronavirus disease 2019 in Wuhan, China. *JAMA Neurol*. 2020;77(6):683–690.
8. Oxley TJ, Mocco J, Majidi S, et al. Large-vessel stroke as a presenting feature of COVID-19 in the young. *N Engl J Med*. 2020;382(20):e60.
9. Poyiadji N, Shahin G, Noujaim D, Stone M, Patel S, Griffith B. COVID-19–associated acute hemorrhagic necrotizing encephalopathy: CT and MRI features. *Radiology*. 2020;296(2):201187.
10. Scheidl E, Canseco DD, Hadji-Naumov A, Bereznai B. Guillain-Barré syndrome during SARS-CoV-2 pandemic: A case report and review of recent literature. *J Peripher Nerv Syst*. 2020;25(2):204–207.
11. Mehta P, McAuley DF, Brown M, et al. COVID-19: Consider cytokine storm syndromes and immunosuppression. *Lancet*. 2020;395(10229):1033–1034.
12. Tang N, Li D, Wang X, Sun Z. Abnormal coagulation parameters are associated with poor prognosis in patients with novel coronavirus pneumonia. *J Thromb Haemost*. 2020;18(4):844–847.
13. Varga Z, Flammer AJ, Steiger P, et al. Endothelial cell infection and endotheliitis in COVID-19. *Lancet*. 2020;395(10234):1417–1418.
14. Zhang Y, Xiao M, Zhang S, et al. Coagulopathy and antiphospholipid antibodies in patients with COVID-19. *N Engl J Med*. 2020;382(17):e38.
15. Li Y, Li H, Fan R, et al. Coronavirus infections in the central nervous system and respiratory tract show distinct features in hospitalized children. *Intervirology*. 2016;59(3):163–169.
16. Zubair AS, McAlpine LS, Gardin T, Farhadian S, Kuruvilla DE, Spudich S. Neuropathogenesis and neurologic manifestations of the coronaviruses in the age of coronavirus disease 2019: A review. *JAMA Neurol*. 2020;77(8):1018–1027.
17. Steardo L, Steardo L Jr., Zorec R, Verkhratsky A. Neuroinfection may contribute to pathophysiology and clinical manifestations of COVID-19. *Acta Physiol (Oxf)*. 2020;229(3):e13473.
18. Andriuta D, Roger PA, Thibault W, et al. COVID-19 encephalopathy: Detection of antibodies against SARS-CoV-2 in CSF. *J Neurol*. 2020;267(10):2810–2811.
19. Asadi-Pooya AA, Simani L. Central nervous system manifestations of COVID-19: A systematic review. *J Neurol Sci*. 2020;413:116832.

20. Benameur K, Agarwal A, Auld SC, et al. Encephalopathy and encephalitis associated with cerebrospinal fluid cytokine alterations and coronavirus disease, Atlanta, Georgia, USA, 2020. *Emerg Infect Dis*. 2020;26(9):2016–2021.
21. Huang C, Wang Y, Li X, et al. Clinical features of patients infected with 2019 novel coronavirus in Wuhan, China. *Lancet*. 2020;395(10223):497–506.
22. Novi G, Rossi T, Pedemonte E, et al. Acute disseminated encephalomyelitis after SARS-CoV-2 infection. *Neurol Neuroimmunol Neuroinflamm*. 2020;7(5):e797.
23. Ye M, Ren Y, Lv T. Encephalitis as a clinical manifestation of COVID-19. *Brain Behav Immun*. 2020;88:945–946.
24. Reichard RR, Kashani KB, Boire NA, Constantopoulos E, Guo Y, Lucchinetti CF. Neuropathology of COVID-19: A spectrum of vascular and acute disseminated encephalomyelitis (ADEM)-like pathology. *Acta Neuropathol*. 2020;140(1):1–6.
25. Duarte-Neto AN, Monteiro RAA, da Silva LFF, et al. Pulmonary and systemic involvement in COVID-19 patients assessed with ultrasound-guided minimally invasive autopsy. *Histopathology*. 2020;77(2):186–197.
26. Remmelink M, De Mendonca R, D'Haene N, et al. Unspecific post-mortem findings despite multiorgan viral spread in COVID-19 patients. *Crit Care*. 2020;24(1):495.
27. Puelles VG, Lütgehetmann M, Lindenmeyer MT, et al. Multiorgan and renal tropism of SARS-CoV-2. *N Engl J Med*. 2020; 383(6):590–592.
28. Solomon IH, Normandin E, Bhattacharyya S, et al. Neuropathological features of COVID-19. *N Engl J Med*. 2020; 383(10):989–992.
29. Wichmann D, Sperhake JP, Lutgehetmann M, et al. Autopsy findings and venous thromboembolism in patients with COVID-19: A prospective cohort study. *Ann Intern Med*. 2020; 173(4):268–277.
30. Lengfeld JE, Lutz SE, Smith JR, et al. Endothelial Wnt/β-catenin signaling reduces immune cell infiltration in multiple sclerosis. *Proc Natl Acad Sci U S A*. 2017;114(7):e1168–e1177.
31. Santoriello D, Khairallah P, Bomback AS, et al. Postmortem kidney pathology findings in patients with COVID-19. *J Am Soc Nephrol*. 2020;31(9):2158–2167.
32. Montine TJ, Phelps CH, Beach TG, et al.; National Institute on Aging; Alzheimer's Association. National Institute on Aging-Alzheimer's Association guidelines for the neuropathologic assessment of Alzheimer's disease: A practical approach. *Acta Neuropathol*. 2012;123(1):1–11.
33. Meinhardt J, Radke J, Dittmayer C, et al. Olfactory transmucosal SARS-CoV-2 invasion as a port of central nervous system entry in individuals with COVID-19. *Nat Neurosci*. 2021;24(2):168–175.
34. McKie AM, Jones TPW, Sykes C. Prolonged viral shedding in an immunocompetent patient with COVID-19. *BMJ Case Rep*. 2020;13(10):e237357.
35. Wölfel R, Corman VM, Guggemos W, et al. Virological assessment of hospitalized patients with COVID-2019. *Nature*. 2020; 581(7809):465–469.
36. Hanley B, Naresh KN, Roufosse C, et al. Histopathological findings and viral tropism in UK patients with severe fatal COVID-19: A post-mortem study. *Lancet Microbe*. 2020;1(6):e245–e253.
37. Al-Dalahmah O, Thakur KT, Nordvig AS, et al. Neuronophagia and microglial nodules in a SARS-CoV-2 patient with cerebellar hemorrhage. *Acta Neuropathol Commun*. 2020;8(1):147.
38. Al-Sarraj S, Troakes C, Hanley B, et al. Invited review: The spectrum of neuropathology in COVID-19. *Neuropathol Appl Neurobiol*. 2020;47(1):3–16.
39. Jensen MP, Le QJ, Officer-Jones L, et al. Neuropathological findings in two patients with fatal COVID-19. *Neuropathol Appl Neurobiol*. 2021;47(1):17–25.
40. Matschke J, Lutgehetmann M, Hagel C, et al. Neuropathology of patients with COVID-19 in Germany: A post-mortem case series. *Lancet Neurol*. 2020;19(11):919–929.
41. Vinters HK-D. General pathology of the central nervous system. In: Love SPA, Ironside J, Budka H, eds. *Greenfield's neuropathology*, 9th ed. CRC Press; 2015:32–33.
42. Garber C, Soung A, Vollmer LL, et al. T cells promote microglia-mediated synaptic elimination and cognitive dysfunction during recovery from neuropathogenic flaviviruses. *Nat Neurosci*. 2019;22(8):1276–1288.
43. Brown GC, Neher JJ. Microglial phagocytosis of live neurons. *Nat Rev Neurosci*. 2014;15(4):209–216.
44. Lemstra AW, Groen in't Woud JC, Hoozemans JJ, et al. Microglia activation in sepsis: A case-control study. *J Neuroinflammation*. 2007;4:4.
45. Tröscher AR, Wimmer I, Quemada-Garrido L, et al. Microglial nodules provide the environment for pathogenic T cells in human encephalitis. *Acta Neuropathol*. 2019;137(4):619–635.
46. Jubelt B, Mihai C, Li TM, Veerapaneni P. Rhombencephalitis/brainstem encephalitis. *Curr Neurol Neurosci Rep*. 2011;11(6):543–552.
47. Vasek MJ, Garber C, Dorsey D, et al. A complement-microglial axis drives synapse loss during virus-induced memory impairment. *Nature*. 2016;534(7608):538–543.
48. Nauen DW, Hooper JE, Stewart CM, Solomon IH. Assessing brain capillaries in coronavirus disease 2019. *JAMA Neurol*. 2021;e210225.
49. Mukerji SS, Solomon IH. What can we learn from brain autopsies in COVID-19? *Neurosci Lett*. 2021;742:135528.
50. Lee MH, Perl DP, Nair G, et al. Microvascular injury in the brains of patients with COVID-19. *N Engl J Med*. 2021;384(5):481–483.